Interferometry for fermionic atoms with transverse momentum

Tun Wang and Juha Javanainen
Department of Physics, University of Connecticut, Storrs, Connecticut 06269, USA
(Received 28 August 2006; published 4 January 2007)

An interferometer using fermions with transverse momentum is analyzed. It is shown that the phase uncertainty $\Delta\theta$ of such a fermion interferometer with either two-dimensional (2D) or one-dimensional (1D) transverse momentum states can be lower than that of an interferometer using fermions with the longitudinal momentum state. The improvement is due to the fact that the transit time for the transverse momentum states is a constant and thus the phase evolution factor is a quadratic function of the dispersive momentum compared to the linear dependence of phase evolution on the dispersive momentum for the longitudinal momentum state. Furthermore, 2D transverse momentum state may have lower phase uncertainty than 1D transverse momentum state because of dimensional effects.

DOI: 10.1103/PhysRevA.75.013605 PACS number(s): 03.75.Hh, 03.75.Dg, 05.30.−d, 07.60.Ly

In recent years ultracold atomic gases have been successfully employed to perform high-precision interferometry [1–7]. Atom interferometers offer a potential sensitivity that exceeds that of their optical counterparts by as much as $Mc^2/\hbar\omega \sim 10^{10}$ [8,9]. Theoretical analysis of the sensitivity of atom interferometers has shown that phase uncertainty of matter-wave Mach-Zehnder interferometer for uncorrelated inputs is $1/\sqrt{N}$, while correlated inputs can achieve the Heisenberg limit $\sim 1/N$ [10,11]. These are true when the atomic beam is quasi-monochromatic [9,11,12]. The quasi-monochromatism is justified when the atomic wave functions do not overlap, which means quantum statistics does not play a role and thus bosons and fermions give the same result.

Clearly, to decrease phase uncertainty, increasing N is desired, which will make the wave functions of different atoms overlap when N is large. Thus treatment with quantum statistics of atoms is necessary, and bosons and fermions will give different results. For bosonic atoms, the interference pattern and phase sensitivity is degraded because of the atom-atom interactions, which give rise to a nonlinear phase shift as the atoms propagate along the arms of the interferometer. For identical fermions, although there is no s-wave collisions between degenerate identical fermions, one still might expect that the phase sensitivity is also degraded, since they have different momentum according to Pauli exclusion principle [13]. However, Search and Meystre [14] have shown that for fermions, the phase uncertainty of a Mach-Zehnder interferometer using a degenerate beam of fermions can be noticeably smaller than what can be achieved by using BEC or nonoverlapping wave functions. The lowering of noise for the fermions can be attributed to the antibunching of the fermions between the two arms of the interferometer. Successive fermions entering the interferometer will have a greater probability of being found in different arms of the interferometer rather than in the same arm as would be the case for bosons. On the other hand, this antibunching is modified by the broadband (or "white light") nature of the Fermi gas in k space, which limits the range of the measured phases over which the phase uncertainty is improved.

All the analysis [9,11,12] so far considers an effective one-dimensional system: the motion of atoms transverse to the interferometer arms is ignored. In this paper, we will show that atoms with transverse momentum can decrease the phase uncertainty of a single-port-input Mach-Zehnder interferometer. In the following, a short review of the atomic Mach-Zehnder interferometer with atoms having longitudinal momentums is presented first. It is followed by showing that both two-dimensional and one-dimensional transverse momentum states can reduce the phase uncertainty of the interferometer. It is then followed by the discussion and conclusion.

Figure 1 shows the atomic Mach-Zehnder interferometer that we consider, with input ports A and B. We introduce the annihilation (creation) operators $\hat{a}_{\vec{k}}$ ($\hat{a}^\dagger_{\vec{k}}$) and $\hat{b}_{\vec{k}}$ ($\hat{b}^\dagger_{\vec{k}}$) for atoms entering the input ports A and B, respectively, with momentum $\hbar k_z$ directed along either the upper or lower interferometer path, each of which defines a z direction of its own. $\hat{a}_{\vec{k}}$ and $\hat{b}_{\vec{k}}$ satisfy anticommutation relations $[\hat{a}_{\vec{k}}, \hat{a}^\dagger_{\vec{k}'}]_+ = \delta_{\vec{k},\vec{k}'}$ and $[\hat{b}_{\vec{k}}, \hat{b}^\dagger_{\vec{k}'}]_+ = \delta_{\vec{k},\vec{k}'}$, respectively. The beam splitters 1 and 2 are both 50/50 beam splitters, and, e.g., the first one has the action

$$\begin{pmatrix} \hat{a}_{u,\vec{k}} \\ \hat{a}_{l,\vec{k}} \end{pmatrix} = \frac{1}{\sqrt{2}} \begin{pmatrix} i & -1 \\ -1 & i \end{pmatrix} \begin{pmatrix} \hat{a}_{\vec{k}} \\ \hat{b}_{\vec{k}} \end{pmatrix}, \tag{1}$$

here $\hat{a}_{u,\vec{k}}(\hat{a}_{l,\vec{k}})$ are the operators for the upper (lower) paths of the interferometer. We assume that, upon reflection from a beam-splitter surface, the atoms undergo an unimportant phase shift which we take to be $\pi/2$, and upon passage

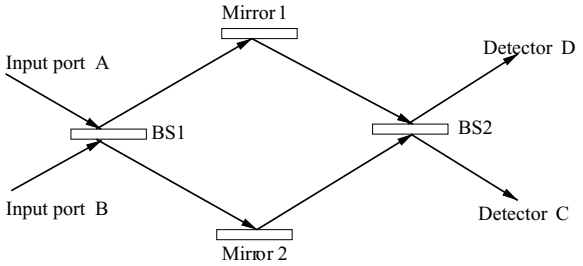

FIG. 1. Mach-Zehnder interferometer. l_u and l_l are the path lengths for the upper and lower arms, respectively. BS1 and BS2 are 50/50 beam splitters.

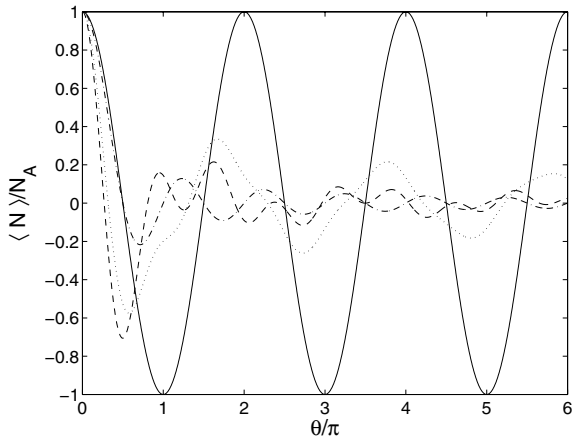

FIG. 2. Dimensionless differential number $\langle N\rangle/N_A$ as a function of phase difference θ for ideal single momentum state (solid line), fermions with the longitudinal state $|\Psi\rangle_z$ (dashed-dotted line), fermions with the XY transverse momentum state $|\Psi\rangle_{XY}$ (dashed line) and fermions with the X transverse momentum state $|\Psi\rangle_x$ (dotted line). Reduced contrast for momentum broadened states, which is due to Pauli's principle, can be clearly seen. But for fermions, $\langle N\rangle/N_A$ drops faster, which means smaller phase uncertainty. In the plot, $\bar{n}_A=2$, $r=1.31$ ($r=1.32$) for the XY (X) transverse state are used.

through a beam splitter, the atoms undergo zero phase. After the beams are recombined at the second beam splitter, the atoms are counted by detectors located at the output ports C and D. The observable is the difference in the numbers of counts

$$\hat{N}=\hat{N}_C-\hat{N}_D=\sum_{\vec{k}}(\hat{c}_{\vec{k}}^{\dagger}\hat{c}_{\vec{k}}-\hat{d}_{\vec{k}}^{\dagger}\hat{d}_{\vec{k}}), \tag{2}$$

where $\hat{c}_{\vec{k}}$ and $\hat{d}_{\vec{k}}$ are the annihilation operators for the output ports C and D, respectively. We call $\hat{N}$ the differential number operator and $\langle\hat{N}\rangle$ the differential number. For single port input ($\langle b_{\vec{k}}^{\dagger}b_{\vec{k}}\rangle=0,\langle a_{\vec{k}}^{\dagger}a_{\vec{k}}\rangle=N_{A,\vec{k}}$) which we consider in this paper, the differential number becomes

$$\langle\hat{N}\rangle=\sum_{\vec{k}}\langle a_{\vec{k}}^{\dagger}a_{\vec{k}}\rangle\cos\,\omega_k t_0, \tag{3}$$

where

$$\hbar\omega_k=\hbar^2(k_x^2+k_y^2+k_z^2)/2m \tag{4}$$

is the energy of a fermion of mass m with momentum $\hbar\vec{k}=\hbar(k_x,k_y,k_z)$, and

$$t_0=m\Delta l/\hbar k_z \tag{5}$$

is its time to travel through the two arms, and Δl is the path length difference between the upper and lower arms of the interferometer. For clarity, $a_{\vec{k}}$ will be specified for different states [see Eqs. (7), (11), and (14)]. The phase uncertainty in a Mach-Zehnder interferometer is defined as [14]

$$\Delta\theta=\Delta N/|\partial\langle\hat{N}\rangle/\partial\theta| \tag{6}$$

with $\Delta N=(\langle\hat{N}^2\rangle-\langle\hat{N}\rangle^2)^{1/2}$. In the following, the vector in $\vec{k}$ will be suppressed for simplicity. Before we proceed to specific states, we stress the key difference of different states. When Eqs. (4) and (5) are substituted into Eq. (3), we see that without transverse momentum broadening ($k_x=k_y=0$), the phase factor for mode $\vec{k}$ is linear in k_z; while for case without longitudinal momentum broadening ($k_z=k_0$ are constants), the phase factor is quadratic in k_x and k_y. This difference together with its counterpart in the expression of ΔN, as will be shown in the following, can reduce the phase uncertainty of states with transverse momentum broadening ($k_x\neq 0$ and/or $k_y\neq 0$).

Longitudinal momentum state. When the momentum broadening is along the z axis, as was considered in Refs. [12,14], the quantum state for the incident fermions at zero temperature is given by

$$|\Psi\rangle_z=\Pi_{|k_z-k_0|\leqslant k_F}\hat{a}_{k_z}^{\dagger}|0\rangle \tag{7}$$

which will be called as the longitudinal momentum state. Here, $\hbar k_F$ is the one-dimensional Fermi momentum, and $\hbar k_0$ is the average momentum. It can be seen from Eq. (5) that t_0 in Eq. (4) are different for fermions with different momenta. Following Eq. (3), the differential number for $|\Psi\rangle_z$ is

$$\langle\hat{N}\rangle=\frac{L_F}{2\pi}\int_{k_0-k_F}^{k_0+k_F}\cos\left(\frac{\hbar k^2}{2m}\frac{m\Delta l}{\hbar k}\right)dk \tag{8}$$

$$=N_A\cos\,\theta\,\mathrm{sinc}(\bar{n}_A\theta/2), \tag{9}$$

where we defined the function $\mathrm{sinc}(x)=\sin(x)/x$, the phase difference between the two arms for a fermion with average momentum $\hbar k_0$ in the z direction $\theta=k_0\Delta l/2$, dimensionless density $\bar{n}_A=2\pi N_A/L_F$, $k_0=2k_F/k_0$, with L_F being the length of the incident beam. Note that, as seen from Eq. (8), to make the atoms travel from the input to the output, one must make sure that $k_0\geqslant k_F$. Thus we have $\bar{n}_A\leqslant 2$, which was not taken into account in Ref. [14]. Furthermore, it can be seen that N_A cannot be bigger than $N_A^m=2k_oL_F/\pi$ for the interferometer with longitudinal momentum state. Following Eq. (6), the corresponding phase uncertainty $\Delta\theta$ for this state is

$$\sqrt{2N_A}\Delta\theta=\frac{\sqrt{\theta^2[1-\cos\,2\theta\,\mathrm{sinc}(\bar{n}_A\theta)]}}{|\cos\,\theta\cos(\theta\bar{n}_A/2)-\mathrm{sinc}(\bar{n}_A\theta/2)(\theta\sin\,\theta+\cos\,\theta)|}. \tag{10}$$

Note that Eq. (10) is the same as that in Ref. [14] except that our θ is one-half of that in Ref. [14]. Since there is no s-wave interaction between degenerate identical fermions, increasing their density does not cause unfavorable phase shift as bosons do. As was shown in Ref. [14], the larger the dimensionless density $\bar{n}_A$ is, the smaller the phase uncertainty is. This is why fermions are preferable to bosons in atom interferometry [14].

XY transverse momentum state. When the momentum in z is $\hbar k_0$ and the transverse momentum $\hbar k_\perp$ is filled up to Fermi momentum $\hbar k_F$ at zero temperature, the state is

$$|\Psi\rangle_{XY}=\Pi_{|k_\perp|\leqslant k_F}\hat{a}_{k_\parallel}^{\dagger}|0\rangle \tag{11}$$

which will be called the *XY* transverse momentum state in the following. It can be seen from Eq. (5) that t_0 in Eq. (4) are the same for fermions with different transverse momentum in the state $|\Psi\rangle_{XY}$ as well as in the following *X transverse momentum state* $|\Psi\rangle_X$. It follows from Eq. (3) that the differential number for the state $|\Psi\rangle_{XY}$ is

$$\langle\hat{N}\rangle = \left(\frac{L_{xy}^2}{2\pi}\right)\int_0^{k_{xy}} \cos\left(\frac{\hbar(k^2+k_0^2)}{2m}\frac{m\Delta l}{\hbar k_0}\right)kdk$$

$$= N_A\left(\mathrm{sinc}(r^2\theta)\cos\theta + \frac{\cos(r^2\theta)-1}{r^2\theta}\sin\theta\right), \quad (12)$$

where $r=\frac{k_F}{k_0}$ is a parameter comparable to $\bar{n}_A$. However, r can be varied from 0 to ∞ because the transverse momentum is independent of the longitudinal momentum, while $\bar{n}_A$ is limited from 0 to 2 as explained in the section for the longitudinal momentum state. Of course, compared to longitudinal momentum, large transverse momentum in an interferometer makes the straightforward experimental realization of such an interferometer difficult, although there is no physical principle against it. Figure 2 shows that the broadening of the momentum, which is due to the Pauli exclusion principle, makes the contrast of $\langle\hat{N}\rangle$ for state $|\Psi\rangle_{XY}$ smaller than that of atoms with identical momentum. But for fermions, $\langle N\rangle/N_A$ drops faster, which means smaller phase uncertainty $\Delta\theta$ for state $|\Psi\rangle_{XY}$ [Eq. (13)],

$$\sqrt{2N_A}\Delta\theta = \frac{\sqrt{\cos 2\theta\left(1-\mathrm{sinc}(2r^2\theta)-\sin 2\theta\frac{\cos(2r^2\theta)-1}{2r^2\theta}\right)}}{\left|\cos\theta\left(\frac{-1+\cos(r^2\theta)}{r^2\theta}+\frac{\cos(r^2\theta)}{\theta}-\frac{\sin(r^2\theta)}{r^2\theta^2}\right)-\sin\theta\left(\frac{-1+\cos(r^2\theta)}{r^2\theta^2}+\frac{\sin(r^2\theta)}{\theta}+\frac{\sin(r^2\theta)}{r^2\theta}\right)\right|}. \quad (13)$$

While Eq. (13) shows that $\Delta\theta$ scales as $1/\sqrt{N_A}$, Fig. 3(a) quantitatively shows that $\Delta\theta$ does not decrease monotonically as r increases. Rather, $\Delta\theta$ as a function of r and θ has many minima and resonant maxima. Figure 3(b) shows that the phase uncertainty is reasonably low for $\theta\leqslant\pi/3$ and thus we use $\theta=\pi/3$ from now on. For this θ, the minimum occurs at $r=1.31$, which will be used throughout this paper. We also note that the divergent maxima of the phase uncertainty are determined by the denominator in Eq. (6).

Figure 4 shows the comparison of $\Delta\theta$ between the longitudinal momentum state and the *XY* transverse momentum state. Clearly, the *XY* transverse momentum state has smaller phase uncertainty than the longitudinal momentum state. This is mainly due to the fact that the transverse momentum states have constant transit time and thus the phase evolution factor is a quadratic function of the dispersive momentum. Another cause, as will be shown in the next paragraph, is that the broadening of momentum from one dimensional to two dimensional also helps to improve the phase uncertainty. To understand the dimensional effect, we come to the next transverse momentum state.

X transverse momentum state. In this state, the momentum in z direction is $\hbar k_0$, the motion in y is suppressed by a potential [14], and the momentum in x is filled up to Fermi momentum $\hbar k_F$ at zero temperature. Mathematically, the state reads

$$|\Psi\rangle_X = \Pi_{|k_x|\leqslant k_F}\hat{a}_{k_x}^\dagger|0\rangle \quad (14)$$

which is called the *X* transverse momentum state in the following. This state is similar to the state $|\Psi\rangle_{XY}$ with the difference of momentum broadening only in *X* direction. It then follows that the differential number is

$$\langle\hat{N}\rangle = \frac{L_x}{2\pi}\int_{-k_{FX}}^{k_{FX}} \cos\left(\frac{\hbar(k^2+k_0^2)}{2m}\frac{m\Delta l}{\hbar k_0}\right)dk \quad (15)$$

$$= N_A\int_0^1 \cos[(1+r^2k^2)\theta]dk \quad (16)$$

and the phase uncertainty is

$$\sqrt{2N_A}\Delta\theta = \frac{\sqrt{1-\int_0^1\cos[2(1+r^2k^2)\theta]dk}}{\left|\int_0^1\sin[(1+r^2k^2)\theta](1+r^2k^2)dk\right|}. \quad (17)$$

Figures 2 and 3 demonstrate that the *X* transverse momentum state and the *XY* transverse momentum state have very similar r and θ dependence. For $\theta=\pi/3$, however, the former one has a larger phase uncertainty than the *XY* transverse momentum state for the chosen parameters as shown in Fig. 4. This is due to the difference in the density of states. It is obvious from Fig. 4 that all $\Delta\theta$ for fermions are smaller than that of interaction-free boson. And we know from previous work that interaction will even degrade the phase uncertainty of interferometer with boson [14]. The important conclusion for this paper as shown from Fig. 4 is that the phase uncertainty of atomic interferometer can be decreased more by using transverse momentum states than by using longitudinal momentum states.

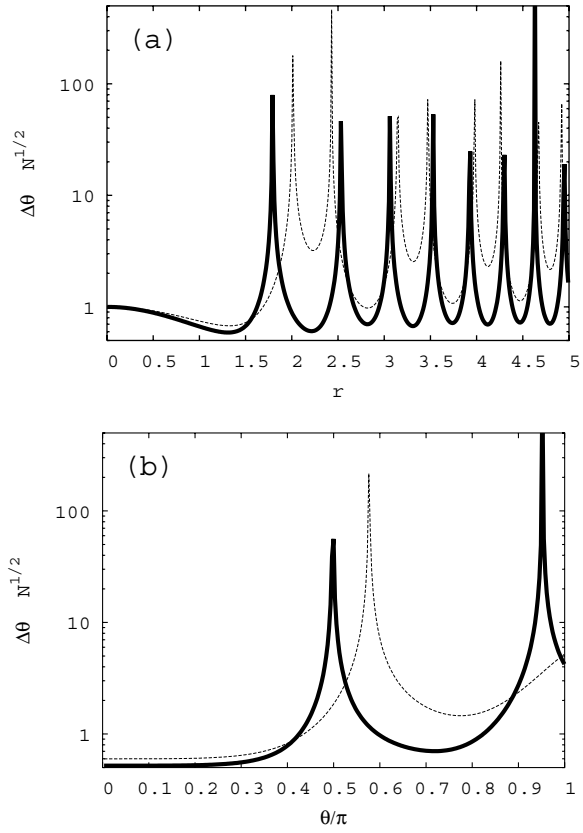

FIG. 3. The phase uncertainty $\sqrt{N_A}\Delta\theta$ for $|\Psi\rangle_{XY}$ (thick line) and $|\Psi\rangle_X$ (thin line) as function of r with $\theta=\pi/3$ (a) and as function of θ with $r=1.31$ ($r=1.32$) for $|\Psi\rangle_{XY}$ ($|\Psi\rangle_X$), (b). Other parameters for the plots are $\bar{n}_A=2$, $r=1.31$ ($r=1.32$) for the XY (X) transverse states.

In Fig. 4, different atom statistics and/or different momentum states are compared by assuming the same total number of atoms N_A through the interferometer. Different from the interferometer with the longitudinal momentum state in which the throughput of atoms N_A has its maximum N_A^m, the interferometer with transverse momentum state has no limitation on N_A. Thus, it is possible to make the phase uncertainty even smaller than that shown in Fig. 4 by increasing N_A with the transverse momentum state.

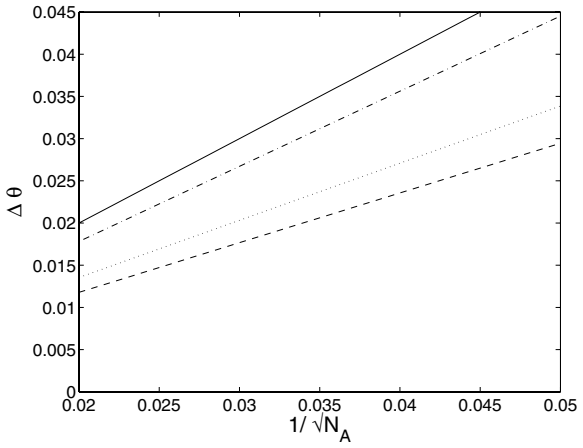

FIG. 4. The phase uncertainty $\Delta\theta$ for interaction-free bosons (thick solid line), the longitudinal momentum state (dashed-dotted line), the XY transverse momentum state (dashed line) and the X transverse momentum state (dotted line). Clearly, the XY transverse momentum state and the X transverse momentum state have smaller phase uncertainty than the longitudinal momentum state. The parameters in plots are $1/\sqrt{N_A}=0.03$, $\theta=\pi/3$, $r=1.31$ ($r=1.32$) for the XY (X) transverse states.

To conclude, transverse motion of atoms as a new twist for reducing the phase uncertainty of atomic interferometer is introduced. The reason for the improvement is that for fermions in the transverse momentum states $|\Psi\rangle_{XY}$ or $|\Psi\rangle_X$, transit time t_0 is a constant, and the phase evolution comes only from the energy spectrum $\hbar\omega_k$, while for longitudinal momentum state $|\Psi\rangle_z$, transit time varies as well, which destructively interferes with $\hbar\omega_k$ to degrade the phase uncertainty. Furthermore, XY transverse momentum state may have lower phase uncertainty than X transverse momentum state because of dimensional effects. Effect of correlated inputs [10,11] using these transverse momentum states on phase uncertainty is under further investigation. The big question that remains is how to realize such a system experimentally.

This work was supported in part by NSF Grant No. PHY-0354599 and NASA Grant No. (NAG3-2880). One of the authors (T. W.) acknowledges the helpful discussions with S. Yelin.

[1] A. Peters, K. Y. Chung, and S. Chu, Nature (London) **400**, 849 (1999).
[2] J. M. McGuirk, G. T. Foster, J. B. Fixler, M. J. Snadden, and M. A. Kasevich, Phys. Rev. A **65**, 033608 (2002).
[3] S. Gupta, K. Dieckmann, Z. Hadzibabic, and D. E. Pritchard, Phys. Rev. Lett. **89**, 140401 (2002).
[4] A. B. Matsko, N. Yu, and L. Maleki, Phys. Rev. A **67**, 043819 (2003).
[5] S. Dimopoulos and A. A. Geraci, Phys. Rev. D **68**, 124021 (2003).
[6] G. Roati, E. de Mirandes, F. Ferlaino, H. Ott, G. Modugno, and M. Inguscio, Phys. Rev. Lett. **92**, 230402 (2004).
[7] B. Dubetsky and M. A. Kasevich, Phys. Rev. A **74**, 023615 (2006).
[8] J. F. Clauser, Physica B & C **151**, 262 (1988).
[9] M. O. Scully and J. P. Dowling, Phys. Rev. A **48**, 3186 (1993).
[10] L. Pezzé and A. Smerzi, Phys. Rev. A **73**, 011801(R) (2006).
[11] J. P. Dowling, Phys. Rev. A **57**, 4736 (1998).
[12] B. Yurke, Phys. Rev. Lett. **56**, 1515 (1986).
[13] G. Roati, E. de Mirandes, F. Ferlaino, H. Ott, G. Modugno, and M. Inguscio, Phys. Rev. Lett. **92**, 230402 (2004).
[14] C. P. Search and P. Meystre, Phys. Rev. A **67**, 061601(R) (2003).